Coalescence efficiency of surface modified PBT meltblown nonwovens in the separation of water from diesel fuel containing surfactants

Hamidreza Arouni [a],[*], Umer Farooq [b], Parikshit Goswami [c], Nikil Kapur [d], Stephen J. Russell [a]

[a] School of Design, University of Leeds, Leeds, LS2 9JT, United Kingdom
[b] Parker Hannifin Manufacturing (UK) Ltd., Dewsbury, WF12 7RD, United Kingdom
[c] Technical Textiles Research Centre, School of Applied Sciences, University of Huddersfield, Huddersfield, HD1 3DH, United Kingdom
[d] School of Mechanical Engineering, University of Leeds, LS2 9JT, United Kingdom

ARTICLE INFO

ABSTRACT

Removal of water from diesel fuel is essential to ensure efficient operation of High-Pressure Common-Rail (HPCR) fuel injection systems used in modern diesel engines. The presence of surfactants in modern fuels (including biofuels) can create conditions in which the interfacial tension between water and fuel is reduced, leading to coalescing media being "disarmed" and less effective in separation. To elucidate this phenomenon in industrially available depth coalescing media, the coalescence efficiency of surface-modified poly (butylene terephthalate) (PBT) meltblown nonwoven fabrics possessing a wide range of wetting behaviours was studied. Tuning of the wettability was accomplished by alkaline hydrolysis of the medium. Using reference grade diesel fuel with and without added surfactants, the coalescence efficiency and quality factor were studied by means of a purpose-built coalescence test rig. The coalescence efficiency was found to depend on both the fuel composition and the wettability of the treated PBT and the optimum efficiency for each test fuel required a difference in wettability of the PBT. For reference grade diesel, increasing the wettability to 'intermediate' level improved coalescence efficiency, but the quality factor can be negatively affected by water droplet retention within the medium. The reduced quality factor associated with hydrophilic media was even more pronounced in fuels containing surfactants due to increased pressure drop and re-emulsification of the fuel in water. These findings highlight the practical challenges that exist in engineering a "universal" coalescing medium suitable for removing water from diesel fuels containing surfactants, based solely on the modulation of fibre wettability and hydrophilicity.

Introduction

High-Pressure Common-Rail (HPCR) fuel injection systems in modern diesel engines are vulnerable to severe damage from corrosion, galling, biological sludge and sediments due to the presence of free water in the fuel systems [1]. Separator filters are therefore required to coalesce the water and remove it from the fuel before it reaches critical components [2,3].

Water is almost insoluble in diesel, but it can combine with fuel as a result of condensation, humidity, or due to conditions under which the fuel is maintained during storage, transfer, and transport from the refinery to the vehicle tank. The function of a water separator is to remove free water droplets emulsified in diesel fuel before reaching the injection system, while maintaining optimum flow and a low pressure drop across the medium [4]. From the late 1990's, water separation systems have developed rapidly to meet the needs of Original Equipment

Manufacturers (OEMs), with high efficiencies of >95% being achieved to ensure the total water content of the fuel is kept below 200 ppm [4].

Water separators commonly adopt one of two separation mechanisms, and the use of nonwoven fabrics is important in both approaches [5–8]: (a) single stage separation involving a hydrophobic barrier medium to separate water droplets by surface filtration or, (b) double stage separation in which water droplets are first captured and coalesced in a depth coalescing medium followed by a hydrophobic barrier medium on the downstream side to separate enlarged water droplets from the fuel stream. Commercially, double stage water separation is most attractive because of the superior coalescence efficiency that is possible using high surface area of the depth coalescing media [8].

Commonly, the quality Factor, QF (Equation 1), is used to evaluate water separation performance [3,5,7,9–11]. This index reflects the separation efficiency, e, as well as the pressure drop, ΔP, of the coalescing medium. One of the main challenges water separators encounter is

---

maintenance of low pressure drop across the medium combined with high separation efficiency [3,5,7,9–11]. Normally one is sacrificed to improve the other.

$$QF = \frac{-\ln(1-e)}{\Delta P}$$

Equation 1: Quality factor.

Different approaches have been explored to address the dependency of pressure drop and coalescence efficiency such as varying wetting characteristics and polymer selection, inclusion of submicron fibres and nanofibres [11–14] and modification of geometric structure [11,13, 15–18]. Among these techniques, modifying the surface wettability of fibres has received particular attention [3,5–7,9,10,19–22]. The surface energy of a fibrous medium directly affects adhesion, spreading, and capillary behaviour of dispersed liquid droplets. One common strategy to increase coalescence efficiency in fibrous media such as nonwovens is modification of fibre surface chemistry to increase hydrophilicity.

Kulkarni et al. [10] modified the overall hydrophilicity of the medium by sandwiching layers of PET and PP microfibre with glass microfibers layers, wherein all the samples comprised inlet and outlet layers made of glass fibres. Wettability was characterised by the L/H ratio (lipophilicity/hydrophilicity). At a face velocity of about 8.8 mm/s, they reported L/H ratios of between 310 and 25 to be the optimum values of hydrophilicity in terms of quality factor for glass/PP and glass/PET layered media, respectively. In other work, Kulkarni et al. [20] combined the effects of fibre size and wettability by blending electrospun PP fibres with glass microfibres and examined performance at a face velocity of ~ 8.8 mm/s. They suggested a preferred L/H range of 0.9–1.2 to avoid excessive pressure drop using PP fibres with an average diameter between 300 and 900 nm. Patel et al. [19,23] explored the contribution of a hydrophobic inlet layer on the quality factor of glass fibre substrates in the separation of water from ULSD fuel at different face velocities of 0.33, 0.67, and 1 mm/s. Their work concentrated on electrospun poly (vinylidene fluoride-co-hexafluoropropylene) (PVDF-HFP) media with an average fibre diameter of 334 nm, as well as electrospun PP submicron fibres with average diameters of 876, 1082, and 1710 nm, as inlet layers. They reported that such hydrophobic nanofibrous layers improve the quality factor of glass filter media, although there was a reduction in the total porosity of the medium; a reduction in the quality factor was observed as the face velocity increased. In other work, Rajgarhia et al. [22] reported a significant increase in the quality factor of glass fibre media coated with a hydrophobic nanofibrous layer at a face velocity of 0.33 mm/s based on a mean droplet size of 20 μm. Krasinski et al. [21] also claimed that a hydrophobic PP meltblown inlet layer performs better than a hydrophilic glass fibre inlet layer due to more effective deposition of the coalesced droplets. They also suggested that an electrostatic charge on the hydrophobic inlet layer improved overall efficiency.

Although surface modification of fibrous media and intermediate wettability are potentially promising methods of controlling the quality factor, it is doubtful whether such an approach can deliver a 'universal' coalescing medium when the diesel fuel also contains surfactants. Accordingly, the aim of the present study was to elucidate the performance of a current depth coalescing medium comprising poly (butylene terephthalate) (PBT) meltblown nonwoven in terms of coalescence efficiency and quality factor, as a function of wettability using modern diesel fuels with and without surfactants. Wettability was systematically modulated by means of alkaline hydrolysis [24] and characterised by the L/H ratio [10]. The coalescence efficiency and the quality factor were studied using a purpose-built coalescence test rig using both reference grade diesel (REF), and blends containing 200 ppm (v/v) of the surfactant monoolein (Sigma® 1-Oleoyl-rac-glycerol), (M200).

Materials and experimental methods

Nonwoven coalescing media and fabric characterisation methods

Flat fabric samples of 100% poly (butylene terephthalate) (PBT) meltblown fabric (MB) were supplied by Parker Hannifin Manufacturing (UK) Ltd – Racor Division. To modify the wettability, samples were first cut into squares of 20 cm × 20 cm, and then in to discs with a diameter of 11 cm prior to water separation experiments. The basic properties of the meltblown samples were characterised according to the standard procedures given in Table 1.

Air permeability measurements were made at a fixed pressure of 200 Pa based on a 20 cm^2 test head. The pore size distribution was determined via the Wet up-Dry up procedure. Mean fibre diameter was determined from SEM images and image analysis (Image-Pro). In real filtration and separation systems, coalescing media is subjected to fluid flow that applies multiaxial, rather than uniaxial forces to the fabric structure, and bursting strength is therefore a valuable assessment of mechanical stability. Data were analysed using single factor ANOVA and T-testing, based on at least five replicates per sample.

Preparation of fuel test liquids

Additive-free reference grade diesel (REF, CEC RF-06-03 diesel - Hess Corporation, Germany), and a blend (M200) made from the same reference grade diesel and 200 ppm (v/v) monoolein (1-(cis-9-Octadecenoyl)-rac-glycerol with a density of 969 kg/m^3 Sigma Aldrich UK) were used as test fuels throughout. Specifications of the test fuel liquids are summarised in Table 2.

Fibre surface modification

The wetting behaviour of PBT meltblown fabric samples was modified by alkaline hydrolysis [24]. In this modification, PBT meltblown fabric is submerged in sodium hydroxide (NaOH)/methanol solution such that the polymer is modified by hydroxide ions (OH^-) released in the solution and carboxyl or hydroxyl end groups are formed resulting in improved hydrophilicity [24–26]. In contrast to coating or plasma treatment [27–29], this method of alkaline hydrolysis ensures treatment

Table 1
Nonwoven characterisation procedures.

Property	Unit	Standard No.	Testing Instrument
Area Density (GSM)	$g.m^{-2}$	BS EN 29073-1:1992	METTLER TOLEDO balance
Thickness	mm	BS ISO 9073-2:1996	THWING-ALBERT gage
Air Permeability	$l.m^{-2}.s^{-1}$	EDANA 140.1–81	LabAir FX3300
Pore size –Bubble point	μm	ASTM F316	Capillary flow porometry®
Pore size –Mean flow	μm	ASTM F316	Capillary flow porometry®
Fibre diameter	μm	SEM imaging	JEOL JSM-6610 LV
Bursting strength	kPa	ISO 13938-2:1999	James Heal Burst Tester

Table 2
Test diesel fuel characteristics.

Property	REF	M200	water	Testing Instrument
Water content, ppm (v /v)	49.13 ± 2.79	50.28 ± 4.45	–	Mettler-Toledo-C20 Compact Karl Fischer ISO 760:1978)
Interfacial tension, mN/m	31.24 ± 0.73	18.8 ± 0.21	71.2	Kruss K20 force tensiometer ISO 6889:1986)
Dynamic viscosity, mPa.s	3.43	3.43	0.9	BTI® viscometer -BS/ U-tube, size B ISO 3104:1996)
Density, kg/m³	829.1	829.1	997.6	25 ml Capillary-stoppered pycnometer ISO 3838:2004)

Table 3
Sample codes for the hydrolysis test conditions.

Sample ID	NaOH concentration (mol/l)	Treatment bath temperature T (°C)	Description
MB	N/A	N/A	Untreated sample
MB-0M-40C	0	40	No alkali-treated but exposed to the treating conditions
MB-0.25M-40C	0.25	40	Alkali-treated – 0.25 mol/l NaOH at 40°C
MB-1M-40C	1	40	Alkali-treated – 1 mol/l NaOH at 40°C
MB-3M-35C	3	35	Alkali-treated – 3 mol/l NaOH at 35°C
MB-3M-40C	3	40	Alkali-treated – 3 mol/l NaOH at 40°C

of fibres through the full thickness of the medium takes place.

The hydrolysis treatment bath was prepared by dissolving different concentrations of NaOH into solutions of methanol (50% v/v) and deionised water (50% v/v). PBT fabric samples were cut into squares of 20 cm × 20 cm, and then immersed in the treatment bath for 10 min without stirring (liquor ratio of 1:100). The bath temperature (T) was maintained at 40 °C for NaOH concentrations of 0.25, 1, and 3 mol/l, or 35 °C for a NaOH concentration of 3 mol/l. Three replicates per sample were prepared. Sample codes corresponding to each condition are listed in Table 3, e.g. MB-0.25M-40C refers to fabrics treated at 40 °C with 0.25 mol/l NaOH solution.

The bath temperature was maintained during treatment using temperature control equipment consisting of a thermocouple, PID controller, and a hotplate. Samples were washed after treatment by immersion in distilled water for 60 min (liquor ratio of 1:5000), then quickly immersed in HCl solution (0.1 mol/l - liquor ratio of 1:100), and then samples were rinsed
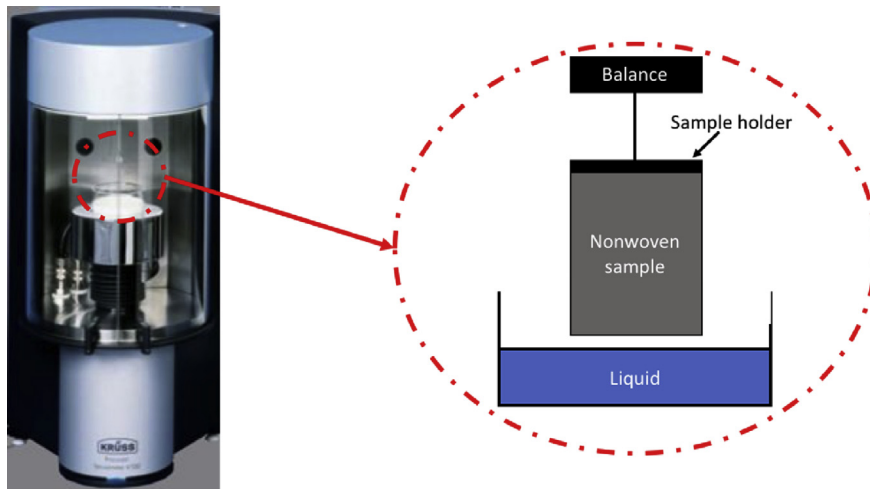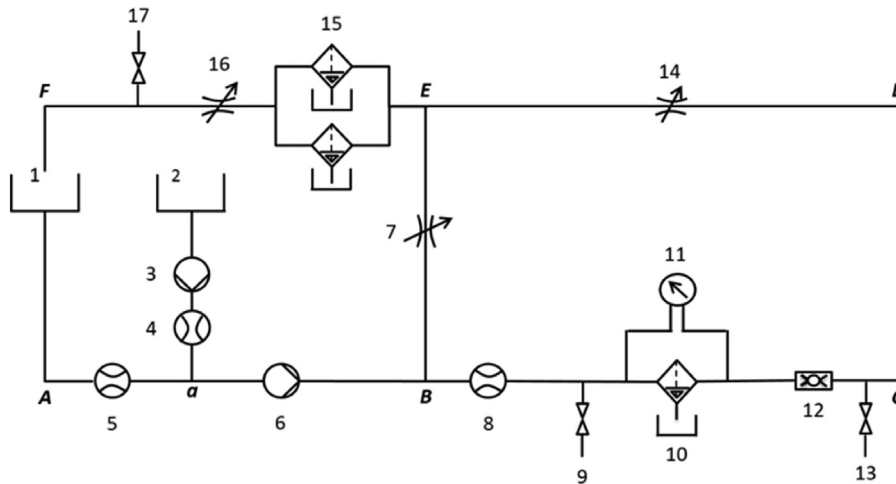

Fig. 1. Tensiometry test setup for obtaining wetting curves of filter media.

1- Fuel tank

2- Water tank

3- Water pump

4, 5, 8- Flow meter

6- Main pump

7,14- Adjustable valve

9, 13, 17- Sampler unit

10- Filter housing

11- Monometer

12- Static mixer

15- Two parallel clean-up filters

16- Pressure valve

Fig. 2. Simple schematic of the coalescing efficiency test rig.

Table 4
Structural properties of the PBT meltblown media.

ID.	Area Density ($g.m^{-2}$)	Thickness (mm)	Air Permeability $l.m^{-2}.s^{-1}$)	Pore size – Bubble point (μm)	Pore size – Mean flow (μm)	Fibre diameter (μm)
MB	228.3 ± 2.14	2.65 ± 0.04	119.42 ± 1.50	33.63 ± 1.17	8.77 ± 0.19	3.58 ± 0.35
MB-0M-40C	225.34 ± 0.11	2.95 ± 0.04	130.1 ± 3.45	34.27 ± 1.81	8.6 ± 0.28	3.09 ± 0.24
MB-0.25M-40C	229.35 ± 1.25	3.13 ± 0.05	132.8 ± 2.98	35.9 ± 0.95	8.45 ± 0.10	3.62 ± 0.28
MB-1M-40C	231.26 ± 4.91	3.25 ± 0.18	137.67 ± 5.36	34.42 ± 1.01	8.86 ± 0.14	3.49 ± 0.20
MB-3M-40C	232.52 ± 10.98	2.92 ± 0.18	137.5 ± 16.39	34.06 ± 1.28	8.89 ± 0.17	3.55 ± 0.27
MB-3M-35C	237.05 ± 5.80	2.95 ± 0.19	132.25 ± 3.30	34.36 ± 2.21	9.02 ± 0.10	3.61 ± 0.19

after being repeatedly immersed in distilled water for 30 min (liquor ratio of 1:5000) until a pH of supernatant reached to 7. Finally, samples were dried in air for 24 h, followed by vacuum drying overnight at 20 °C.

Wettability characterisation technique

The wettability of each sample was characterised by the L/H ratio in accordance with Kulkarni et al. [10], based on the modified Washburn's equation, Equation 2.

$$L\left/H = \frac{S_o \eta_o \rho_w^2 \gamma_w}{S_w \eta_w \rho_o^2 \gamma_o}\right.$$

Equation 2: Modified Washburn's equation (subscript "*o*" refers to oil and "*w*" refers to water).

η, γ, and ρ in Equation 2 denote viscosity, surface tension, and density of the penetrating liquid respectively, and S, Equation 3, is the slope of the wetting curve (W^2 - t), Equation 4, plotting squared mass, (g^2), of the penetrating liquid at time t, where c is the wetting constant. The W^2 - t curve is generated experimentally by conducting a liquid absorption test using tensiometry.

$$S = \frac{c\, \rho^2\, cos\theta\, \gamma}{\eta}$$

Equation 3: Wetting kinetics of a porous medium

$$W^2 = \frac{c\, \rho^2\, cos\theta\, \gamma}{\eta} t$$

Equation 4: Wetting curve of a porous medium.

Kulkarni et al. [10], developed the W^2 - t curve using Washburn's equation, Equation 5, where r_{eff} is the effective capillary radius in the medium and θ is the advancing contact angle, given the height, h, of liquid penetration into the porous structure is related to the mass, W, of the penetrating liquid according to Equation 6, where ε is the porosity of the medium, A is the cross-sectional area of the medium, and ρ the density of the liquid. The constant c in Equation 3 and Equation 4 refers to the combined effects of the medium's structural properties ($c = \frac{\varepsilon^2 A^2 r_{eff}}{2}$).

$$h^2 = \frac{r_{eff}\, cos\theta\, \gamma\, t}{2\eta}$$

Equation 5: Washburn's equation

$$W = \varepsilon\, \rho\, A\, h$$

Equation 6: Mass of penetrating liquid into a porous medium.

In principle, the L/H ratio is related to the wicking performance of a medium when it is in contact with oil, compared to when it is in contact with water, such that in Equation 7, the terms θ_o and θ_w refer to the advancing contact angles of the oil and water phases.

$$L\left/H = \frac{cos\theta_o}{cos\theta_w}\right.$$

Equation 7: Fundamental equation of the L/H ratio.

Combining Equation 3 and Equation 7 results in Equation 2 where the constant c for the same medium in contact with oil and water (c_o and c_w) are equal and cancel out of Equation 2. The modified Washburn's

Table 5
Bursting strength of the PBT meltblown media.

Sample	Bursting strength (kPa)	Height at burst (mm)	Time to burst (S)
MB	351.73 ± 8.88	19.83 ± 0.39	20.42 ± 0.78
MB-0M-40C	363.2 ± 16.89	19.53 ± 0.19	21.77 ± 0.72
MB-0.25M-40C	351.9 ± 7.53	19.5 ± 0.10	20.27 ± 0.20
MB-1M-40C	350.13 ± 10.86	19.6 ± 0.25	21.17 ± 0.37
MB-3M-40C	349.75 ± 1.50	19.37 ± 0.09	20.1 ± 0.06
MB-3M-35C	348.94 ± 1.95	19.2 ± 0.06	20.1 ± 0.06

equation removes the requirement to measure contact angles and r_{eff}, which is complex and associated with significant errors when dealing with porous/rough surfaces such as those present in fibrous substrates.

A Kruss K100 force tensiometry instrument, Fig. 1, operating in absorption measurement mode was used to plot the wetting curves of the test samples using deionised water and REF diesel fuel. A dry test specimen of 10 mm × 10 mm was suspended on the measuring probe and connected to the balance of the tensiometer.

To commence measurements, the probe was lowered towards a vessel containing 50 ml of the test fuel liquid until the lower edge of the dry sample touched the liquid surface and the balance detected liquid contact (sensitivity of 0.005 gf). Once the surface was detected, the mass of the liquid penetrating the sample was recorded every 2 s for a period of 1 min. At least six specimens from each sample in two groups of three were evaluated. One group was tested using distilled water, and the other one using REF diesel. The slope of each wetting curve was calculated by line fitting the initial wetting profile of the curves. Table 3 lists each of the samples studied.

Coalescence efficiency test procedure

A coalescing test rig equipped with a clean-up loop was used to investigate the impacts of wettability on the coalescence performance of the samples. A schematic of the test rig is shown in Fig. 2. In using the test rig, the samples were cut in to discs of 10 cm in diameter and placed in a filter housing for coalescence efficiency testing using REF and M200 fuels. Measurements were made based on three replicates per sample.

With reference to Fig. 2, water is injected into the main circuit at a concentration of 2500 ppm (v/v) for 20 min and is emulsified in the fuel while passing through the centrifugal pump (RG4000 Stuart (6) at a flow rate of 3.33 ± 0.01 l/min, corresponding to a face velocity of 7 mm/s. The resulting water-in-fuel emulsion is then transported to the filter housing (10) with the coalescing medium presented perpendicular to the flow. The housing has a water drainage port 20 mm downstream of the medium, such that coalesced droplets can be collected in a collection bottle. The coalescing performance depends on the capability of the medium to quickly form droplets that can be effectively removed and collected in the bottle. The test fuel is cleaned before it returns into the fuel tank using two Parker Racor Dmax® clean-up filters in series. The coalescence efficiency, ε, was calculated by Equation 8, where M_{Cd} is total volume of water collected downstream of the element and M_{IU} is total volume of injected water upstream of the medium. The pressure drop across the medium was recorded at the end of each test and the
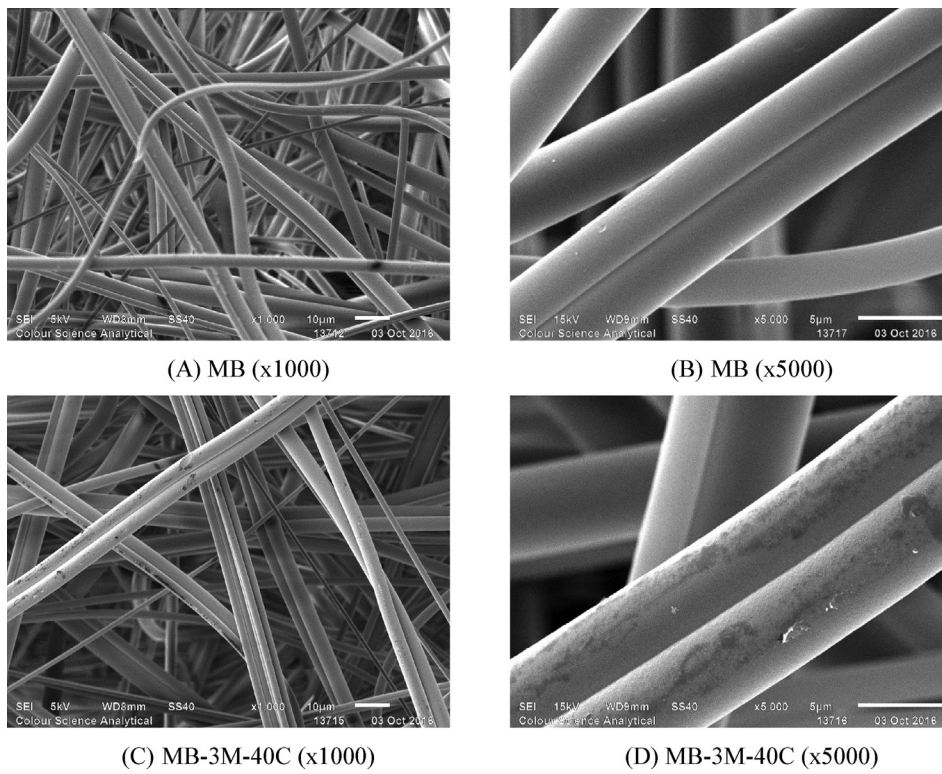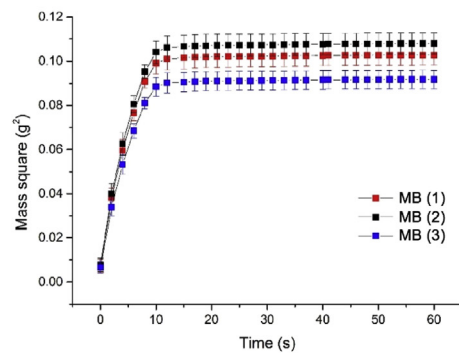
(A) MB (x1000)

(B) MB (x5000)

(C) MB-3M-40C (x1000)

(D) MB-3M-40C (x5000)

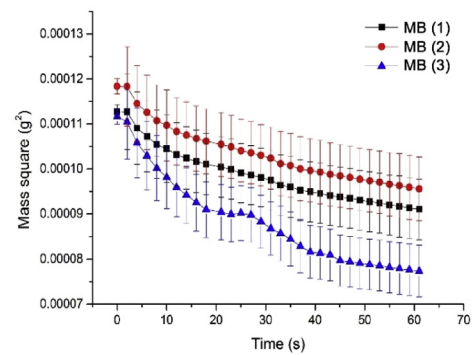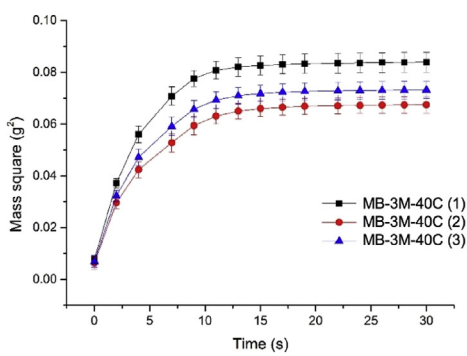**Fig. 3.** SEM images of PBT meltblown media, alkali-treated in 3 mol/l sodium hydroxide at $40.°C$

Fig. 4. Wetting curves of the untreated MB samples in distilled water and REF diesel (see Table 3 for the sample code).

Fig. 5. Wetting curves of the MB-3M-40C in distilled water and REF diesel (see Table 3 for the sample code).

Diesel curves   **Water curves**

Fig. 6. Wetting slope of the untreated MB samples in distilled water and REF diesel (see Table 3 for the sample codes).

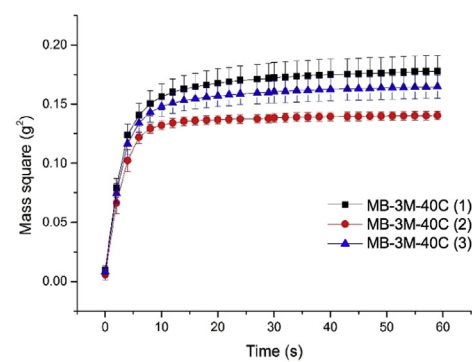**Diesel curves**   **Water curves**

Fig. 7. Wetting slope of the MB-3M-40C in distilled water and REF diesel (see Table 3 for the sample codes).
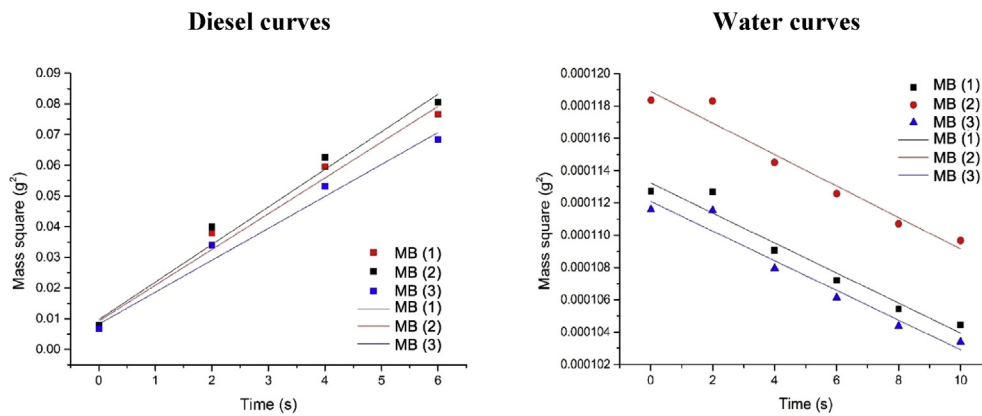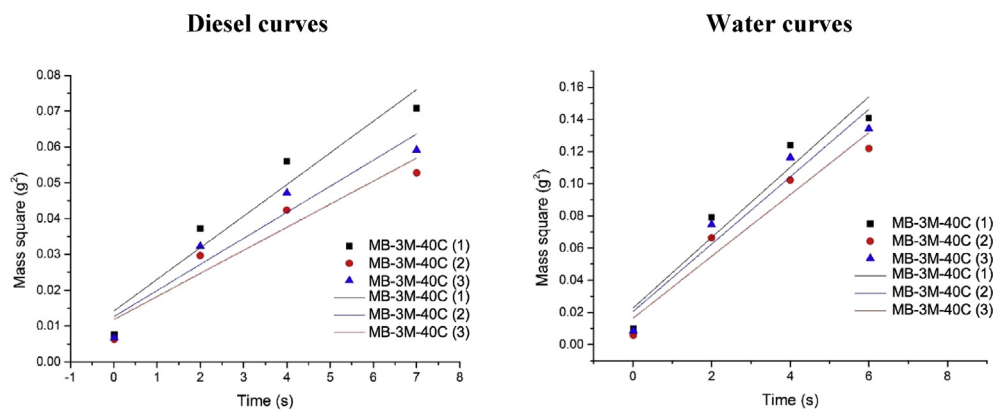
quality factor was calculated using Equation 1.

$$\varepsilon = \frac{M_{Cd}}{M_{IU}}$$

Equation 8: Coalescence efficiency.

Results and discussion

Nonwoven fabric characterisation

Fabric dimensional and physical properties (mean ± SE) are summarised in Table 4 and Table 5.

A single factor ANOVA of the pore size, area density, and bursting strength data of treated and untreated samples revealed no significant differences between the samples (P > 0.05). A t-test analysis of MB and MB-0M-40C showed significant differences in thickness (P = 0.0008) and air permeability (P = 0.004) of the samples at a confidence level of 95%. This was anticipated since no direct changes were made to the geometric configuration of the meltblown samples other than slight dimensional changes over the MB-0M-40C samples due to the treatment procedure,

confirmed by a slight difference in fabric thickness and permeability.

To detect any possible relationship between dimensional changes in alkali-treated samples and coalescence efficiency, data for the alkali-treated samples were analysed by one-way ANOVA, and no significant differences between the MB-0M-40C samples and the other treated samples (P > 0.05) were observed. Furthermore, the SEM images in Fig. 3 revealed no observable physical changes to the surface morphologies of the most intensively treated MB-3M-40C sample (images C and D) compared to its untreated counterpart (images A and B).

Thus, it could be concluded that NaOH-treatment of the samples did not significantly alter the dimensional, geometric or mechanical properties, such that any differences in coalescence performance could be reliably attributed mainly to chemical differences affecting wettability.

3.2. Wettability characterisation

The wettability of the fabrics (listed in Table 3) was characterised according to the methodology explained in Section Wettability characterisation technique and based on six average wetting curves (mean ± SE), i.e. three water curves and three diesel curves, for each

Table 6

L/H values for PBT meltblown media (for IDs see: Table 3, and for parameters see: Equation 2).

ID	S_o	R	S_w	R	L/H
MB	0.01144 ± 0.00054	0.99 ± 0	$-9.4 \times 10^{-7} \pm 0.2 \times 10^{-7}$	0.96 ± 0	<0
MB-0M-40C	0.0132 ± 0.00051	0.97 ± 0	$-4 \times 10^{-6} \pm 0.4 \times 10^{-6}$	0.93 ± 0.04	<0
MB- 0.25M-40C	0.01166 ± 0.00051	0.97 ± 0	0.00016 ± 0.00003	0.95 ± 0.02	918.72231 ± 125.72644
MB-1M-40C	0.01208 ± 0.00213	0.97 ± 0.01	0.00749 ± 0.00147	0.95 ± 0.05	19.92988 ± 0.52352
MB-3M-35C	0.01437 ± 0.00219	0.98 ± 0.01	0.01591 ± 0.00308	0.87 ± 0.01	11.23863 ± 0.46691
MB-3M-40C	0.00752 ± 0.0007	0.93 ± 0.01	0.0207 ± 0.00078	0.94 ± 0.01	4.43312 ± 0.25809
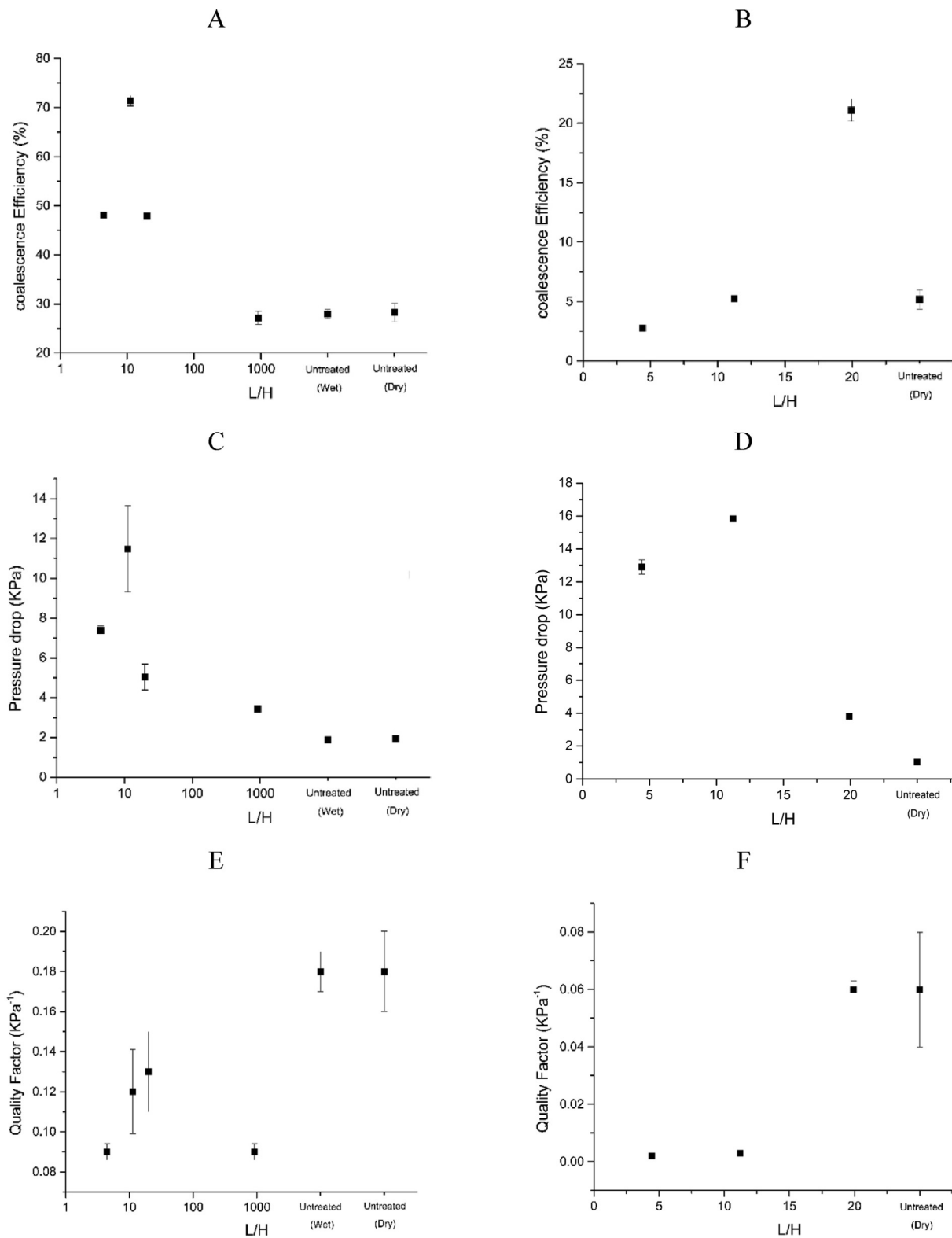
Fig. 8. Effect of wettability on coalescence efficiency, pressure drop, and quality factor of the PBT meltblown media using REF (A, C, and E) and M200 (B, D, and F) fuels; ("Untreated (Wet)" refers to MB samples and "Untreated (Dry)" refers MB-0M-40C samples).

sample. Three replicates were made per sample. Fig. 4 and Fig. 5 show examples of the water and diesel curves for the MB and MB-3M-40C samples. The corresponding wetting slopes in the early part of the process are shown in Fig. 6 and Fig. 7. The slope values and the calculated L/H ratios are reported in Table 6.

The alkaline hydrolysis treatment resulted in a wider range of wetting behaviours in the MB samples (Table 6). The negative and very close to zero L/H ratios for MB and MB-0M-40C are attributable to the hydrophobicity of the PBT media and being pushed away from surface of the liquid during the measurement, which has led to negative readings by the

tensiometer balance and consequently a negative wetting slope. The positive L/H ratios are indicative of a high degree of surface hydrophilicity and wetting propensity in the structure compared the negative L/H ratios. Amongst the positive L/H ratios that were obtained, a smaller value, e.g. 4.3 for MB-3M-40C as compared to 918.72 for MB-0.25M-40C denotes higher hydrophilicity.

3.3. Coalescence efficiency

To understand the relationship between the presence of surfactants and the coalescence efficiency of treated and untreated fabrics, measurements of efficiency were obtained using the REF and M200 fuels according to the methodology explained in Section Coalescence efficiency test procedure. The REF fuel was used for all the treated and untreated samples while testing with the M200 fuel focused on the MB, MB-1M-40C, MB-3M-35C, and MB-3M-40C samples. Fig. 8 reports the coalescence efficiency, pressure drop, and quality factor of the alkaline treated and untreated samples as a function of wettability in the REF and M200 fuels respectively.

With reference to Fig. 8, the coalescence efficiency of MB media using the REF fuel increased at lower L/H ratios (higher hydrophilicity), although the maximum efficiency was obtained at a L/H ratio between 4 and 20 (Fig. 8-A). This is in agreement with the assumption that optimal coalescence is achieved at an "intermediate" hydrophilicity [19,23]. However, it is interesting to note that this was not accompanied by an increase in the quality factor (Fig. 8-E), because of higher pressure drops (Fig. 8-C) due to water retention within the medium. Thus, in practice, increasing the wettability of fibres alone is not a satisfactory approach because of the rise in pressure drop as the optimum hydrophilicity for coalescence is approached (4 < L/H < 20). Moreover, as revealed in Fig. 9, fuel passing through the medium with a high hydrophilicity of fibre surfaces (L/H = 4.43) appeared relatively cloudy compared to the one passing through the medium with an intermediate hydrophilicity (L/H = 11.24), which suggested re-emulsification could take place as

water droplets are expected to be captured efficiently by the medium with higher hydrophilicity.

During the filtration process, the interactions between water droplets and surface treated media can be explained by work of adhesion W_A (Equation 9) and work of spreading, Ws (Equation 10), of the fibre/water interface as well as Laplace pressure (Equation 11) of the droplets in contact with the fibres. Here, γ_{wd}, γ_{fd}, and γ_{fw} are the interfacial tensions (IFT) between the water droplet and diesel, the fibre and diesel, and the fibre and water, respectively. The values of $R1$ and $R2$ are the radii of the curved interface [30,31].

$$W_A = \gamma_{wd} + \gamma_{fd} - \gamma_{fw} \quad or \quad W_A = \gamma_{wd}(1 + \cos\theta)$$

Equation 9: Available work of adhesion

$$Ws = \gamma_{fd} - \gamma_{wd} - \gamma_{fw} \quad or \quad Ws = \gamma_{wd}(\cos\theta - 1)$$

Equation 10: Available work of spreading

$$P_l = \gamma_{lv}\left(\frac{1}{R1} + \frac{1}{R2}\right)$$

Equation 11: Laplace pressure.

Referring to Fig. 10, such media with the ability to enhance coalescence (medium L/H - Fig. 10-C) also promote the formation of large water droplets. This is due to the increased work of adhesion, W_A, as well as work of spreading, Ws, compared to media with low hydrophilicity (high L/H - Fig. 10-A). As a result, water droplets become so well attached that they are not easily removed (Fig. 10-C). In the case of a low L/H ratio (high hydrophilicity - Fig. 10-B), captured droplets tend to spread on the fibre surface resulting in a reduction in their Laplace pressure owing to changes in their surface curvature (Equation 11). Droplets with lowered Laplace pressure exposed to a flowing fuel are vulnerable to the shear stress of the fluid and can be broken and re-emulsified if the stress is higher than their Laplace pressure.

In the presence of surfactant (M200 fuel), and with reference to Fig. 8
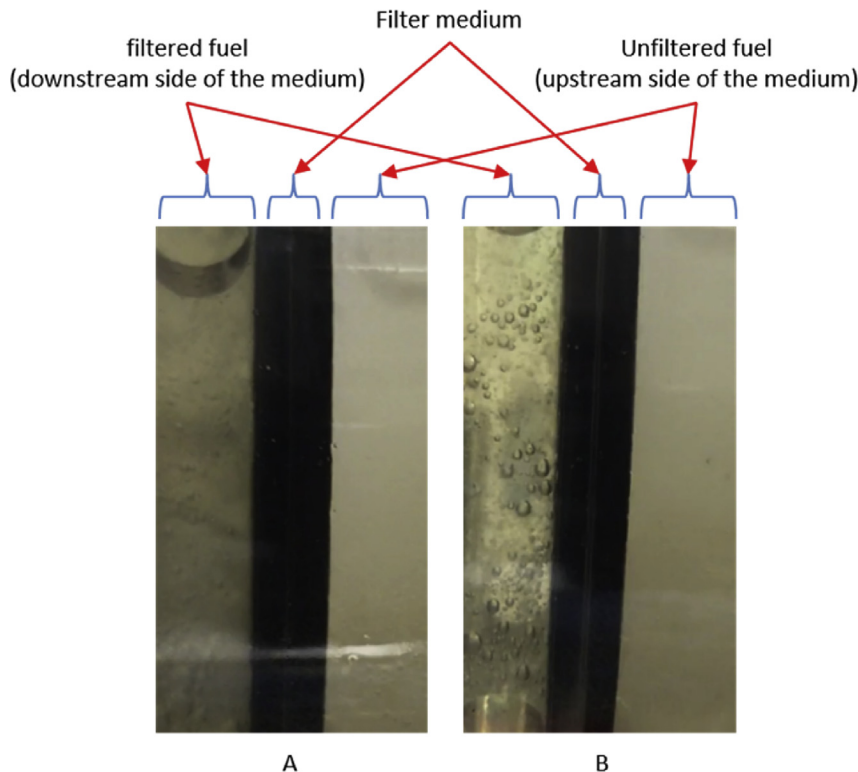
Fig. 9. Cloudiness of REF fuel downstream of (A) sample MB-3M-40C with L/H = 4.43, and (B) sample MB-3M-35C with LH = 11.24 showing that sample A results in a cloudier downstream fluid compared to sample B.
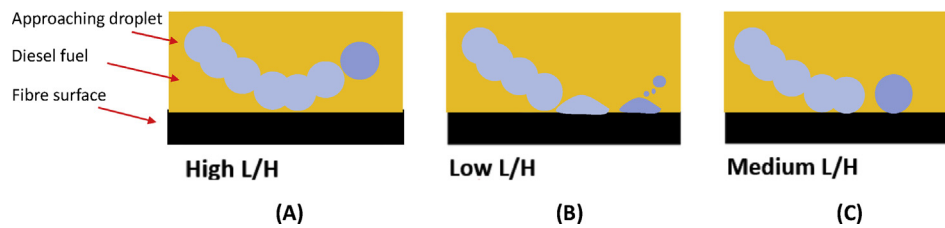
Fig. 10. Schematic of the water droplet interacting with the fibre surfaces of low (A), high (B), and medium (C) hydrophilicity.

(B, D, F), increasing the fibre wettability up to a L/H ratio of 20, results in larger water droplets and an increase in the pressure drop. However, when the hydrophilicity is high, lower coalescence efficiency and an increase in the pressure drop is observed at L/H ratios of 11 and 4. This can be attributed to a sharp increase in both the work of adhesion and the work of spreading within the medium due to an increase in the surface energy of the fibres as a result of hydrolytic surface modification as well as reduction in the interfacial tension of the water droplets as a result of surfactant molecules. This results in retention of water inside the medium, which leads to a greater pressure drop and re-emulsification of small droplets causing low coalescence efficiency.

Comparing the results of the REF and M200 fuels, it can be concluded that the maximum coalescence efficiency for the same coalescing medium is achieved over different hydrophilicity ranges. For the REF fuel, the preferred range is $L/H \approx 11$ and for M200 fuel, the preferred value of $L/H \approx 20$. This highlights the practical challenge that exists in engineering a universally applicable high-performance coalescing medium based solely on the modulation of fibre hydrophilicity.

Conclusions

Wetting behaviour was adjusted independently of the coalescing media's geometric structure to enable systematic study using diesel fuels with and without surfactant content (REF and M200 respectively). The coalescence efficiency and quality factor were determined using a purpose-built coalescence test rig. Although maximum coalescence efficiency could be identified at a particular L/H ratio and hydrophilicity, the quality factor of the untreated (hydrophobic) PBT meltblown medium remained significantly higher (P<0.05) than the hydrophilic variants. The reduction in the quality factor in the case of hydrophilic media was even more pronounced if surfactants were present in the fuel. This was attributed to water being retained within the pore structure of media, resulting in increased pressure drop and re-emulsification of the fuel in water. It was also established that optimal wetting behaviour associated with maximal coalescence efficiency is not the same for REF diesel (free of surfactant) and M200 fuel (containing surfactant). Whilst it has been confirmed that improved coalescence efficiency is achievable for different diesel fuels by tuning the wettability of meltblown PBT media across a specific range of values, reliance on wettability alone is unlikely to provide a basis to design a 'universal' coalescing medium suitable for all diesel fuel compositions.

Conflict of interest

The authors declare that they have no known competing financial interests or personal relationships that could have appeared to influence the work reported in this paper.

Acknowledgements

References

[1] H. Arouni, et al., Limitations of monoolein in simulating water-in-fuel characteristics of EN590 diesel containing biodiesel in water separation testing, SAE Int. J. Fuels Lubr. 11 (3) (2018) 229–238, https://doi.org/10.4271/04-11-03-0012. In press.
[2] A.F. Asmus, B.F. Wellington, Diesel Engines and Fuel Systems, 1995.
[3] F.D. Pangestu, C.M. Stanfel, Media for water separation from biodiesel-ultra low sulfur diesel blends, SAE International Journal of Fuels and Lubricants 2 (1) (2009) 305–316.
[4] M. Petiteaux, G. Monsallier, Impacts of Biodiesel Blends on Fuel Filters Functions, Laboratory and Field Tests Results, 2009. SAE Technical Paper.
[5] C. Stanfel, F. Cousart, Coalescence Media for Separation of Water-Hydrocarbon Emulsions, US Patents, 2008, 2009/0178970.
[6] S. Bansal, et al., Effect of fibrous filter properties on the oil-in-water-emulsion separation and filtration performance, J. Hazard Mater. 190 (1) (2011) 45–50.
[7] L.C. Wadsworth, I.M. Hutten, Handbook of Nonwoven Filter Media, Access Online via Elsevier, 2007.
[8] F.J. Yoshino, et al., Double stage pre-filter diesel water separator, Blucher Engineering Proceedings 2 (1) (2015) 199–207.
[9] R. Brown, T. Wines, Improve suspended water removal from fuels, Hydrocarb. Process. 72 (1993), 95-95.
[10] P.S. Kulkarni, S.U. Patel, G.G. Chase, Layered hydrophilic/hydrophobic fiber media for water-in-oil coalescence, Separ. Purif. Technol. 85 (2012) 157–164.
[11] S.U. Patel, et al., Glass fiber coalescing filter media augmented with polymeric submicron fibers and modified with angled drainage channels, Separ. Purif. Technol. 120 (2013) 230–238.
[12] J. Wang, et al., Manufacturing of polymer continuous nanofibers using a novel co-extrusion and multiplication technique, Polymer 55 (2) (2014) 673–685.
[13] G. Viswanadam, G.G. Chase, Water–diesel secondary dispersion separation using superhydrophobic tubes of nanofibers, Separ. Purif. Technol. 104 (2013) 81–88.
[14] G.G. Chase, Improved Microfiber Filter Performance by Augmentation with Nanofibers, 2007. SAE Technical Paper.
[15] X. Yang, H. Wang, G.G. Chase, Performance of hydrophilic glass fiber media to separate dispersed water drops from ultra low sulfur diesel supplemented by vibrations, Separ. Purif. Technol. 156 (2015) 665–672.
[16] X. Yang, et al., Vibration assisted water-diesel separation by electrospun PVDF-HFP fiber mats, Separ. Purif. Technol. 171 (2016) 280–288.
[17] S.U. Patel, G.G. Chase, Gravity orientation and woven drainage structures in coalescing filters, Separ. Purif. Technol. 75 (3) (2010) 392–401.
[18] S.U. Patel, et al., The effect of surface energy of woven drainage channels in coalescing filters, Separ. Purif. Technol. 87 (0) (2012) 54–61.
[19] S.U. Patel, S.U. Patel, G.G. Chase, Electrospun superhydrophobic poly (vinylidene fluoride-co-hexafluoropropylene) fibrous membranes for the separation of dispersed water from ultralow sulfur diesel, Energy Fuels 27 (5) (2013) 2458–2464.
[20] P.S. Kulkarni, et al., Coalescence filtration performance of blended microglass and electrospun polypropylene fiber filter media, Separ. Purif. Technol. 124 (0) (2014) 1–8.
[21] A. Krasinski, P. Wierzba, Removal of emulsified water from diesel fuel using polypropylene fibrous media modified by ionization during meltblow process, Separ. Sci. Technol. 50 (10) (2015) 1541–1547.
[22] S.S. Rajgarhia, S.C. Jana, G.G. Chase, Separation of water from ultralow sulfur diesel using novel polymer nanofiber-coated glass fiber media, ACS Appl. Mater. Interfaces 8 (33) (2016) 21683–21690.
[23] S.U. Patel, G.G. Chase, Separation of water droplets from water-in-diesel dispersion using superhydrophobic polypropylene fibrous membranes, Separ. Purif. Technol. 126 (0) (2014) 62–68.
[24] Z. Wang, C.W. Macosko, F.S. Bates, Tuning surface properties of poly (butylene terephthalate) melt blown fibers by alkaline hydrolysis and fluorination, ACS Appl. Mater. Interfaces 6 (14) (2014) 11640–11648.
[25] R.R. Mather, R.H. Wardman, Chemistry of Textile Fibres, Royal Society of Chemistry, 2011.
[26] C. Pastore, P. Kiekens, Surface Characteristics of Fibers and Textiles, CRC Press, 2000.
[27] X. Wei, et al., CF 4 plasma surface modification of asymmetric hydrophilic polyethersulfone membranes for direct contact membrane distillation, J. Membr. Sci. 407 (2012) 164–175.
[28] J.P. Fernández-Blázquez, et al., Superhydrophilic and superhydrophobic nanostructured surfaces via plasma treatment, J. Colloid Interface Sci. 357 (1) (2011) 234–238.
[29] E.J. Kim, et al., Preparation of surface-modified poly (butylene terephthalate) nonwovens and their application as leukocyte removal filters, J. Biomed. Mater. Res. B Appl. Biomater. 90 (2) (2009) 849–856.
[30] M.J. Schick, Surface Characteristics of Fibers and Textiles, vol. 7, CRC Press, 1977.
[31] N. Pan, P. Gibson, Thermal and Moisture Transport in Fibrous Materials, CRC Press, 2006.